ELSEVIER

Chemical Engineering Journal 84 (2001) 69–74

Chemical Engineering Journal

www.elsevier.com/locate/cej

Short communication

The assessment of a characteristic drying curve for milk powder for use in computational fluid dynamics modelling

T.A.G. Langrish*, T.K. Kockel

Department of Chemical Engineering, The University of Sydney, Sydney, NSW 2006, Australia

Received 4 March 2000; received in revised form 15 November 2000; accepted 20 November 2000

Abstract

The assessment of a characteristic drying curve for milk powder for use in computational fluid dynamics modelling is reported in this work, for particle sizes and drying conditions typical of those in spray dryers. A review of previous literature, with particle diameters greater than 2 mm, has shown that a linear falling-rate curve is an acceptable approximation for the hindered drying of this material. For the diameters of milk particles in spray dryers, the drying times are predicted using a linear falling-rate curve to be of the order of 1 s compared with residence times of 20–80 s in full-scale equipment.

Keywords: Milk particles; Drying kinetics; Characteristic drying curve; Computational fluid dynamics

1. Introduction

Spray dryers are widely used in the chemical, pharmaceutical and dairy industries, and are the core components of a milk powder production plant, where the basic configuration usually features cocurrent flow of milk powder and air. Significant requirements include reducing both the deposition rate of particles on walls and the time lapse between cleaning cycles, thereby enhancing plant availability. With over 230,000 t manufactured in 1997, the production of skim milk powder is an important sector of the Australian dairy industry, and the production rates of individual spray dryers range from 3 to 28 t of dry powder per hour, so these wall deposition problems are significant.

Although remedial measures, such as air sweeps around walls and hammers at the wall, are possible and are used to reduce these rates [1], another approach is to simulate the air and particle flow patterns inside the chambers in order to understand the deposition process in more detail. This understanding, based on the use of computational fluid dynamics (CFD) techniques, may then be used as the basis to change the patterns (by altering the amount of inlet swirl, for example) so that the deposition rate is reduced. Implicit in such simulations is the need to assess the fate of particles that hit the walls, and the particles only become sticky (and hence adhere to walls) above particular temperatures and moisture contents. Hence, it is necessary to predict the particle temperatures and moisture contents by including a heat and mass-transfer model within these CFD simulations. In this work, we produce such a heat and mass-transfer model. The essential feature of this model is that it is simple and computationally efficient enough to be used in a CFD model, yet faithfully captures the essential features of particle drying.

One possible mass-transfer model is the use of a characteristic drying curve. This approach assumes that, at each volume-averaged free moisture content, there is a corresponding specific drying rate relative to the unhindered drying rate in the first drying period that is independent of the external drying conditions. The relative drying rate is defined as

$$f = \frac{N_V}{\hat{N}_V} \tag{1}$$

where N_V is the drying rate, $\hat{N}_V$ the rate in the first drying period (when the drying rate is limited by the rate of heat transfer to the surface), and the characteristic moisture content is

$$\Phi = \frac{\bar{X} - X_e}{X_{cr} - X_e} \tag{2}$$

where $\bar{X}$ is the volume-averaged moisture content, X_{cr} the moisture content at the critical point, and X_e that at equilibrium. Thus, the drying curve is normalised to pass through

* Corresponding author. Tel.: +61-2-9351-4568.
E-mail address: timl@chem.eng.usyd.edu.au (T.A.G. Langrish).

1385-8947/01/$ – see front matter
PII: S1385-8947(00)00384-3

Nomenclature

A	particle surface area (m^2)
B	constant in Eq. (11) (K^{-1})
C_P	specific heat capacity ($J\,kg^{-1}\,K^{-1}$)
d_P	particle diameter (m)
D_V	diffusivity of water vapour through air ($m^2\,s^{-1}$)
f	relative drying rate (–)
H_V	latent heat of vaporisation of water ($J\,kg^{-1}$)
k	thermal conductivity ($W\,m^{-1}\,K^{-1}$)
K_1, K_2	constants in Eq. (12) ($kg\,kg^{-1}$, –)
m	mass (kg)
M_W	molecular weight ($kg\,mol^{-1}$)
Nu	Nusselt number (–)
N_V	drying rate ($kg\,m^{-2}\,s^{-1}$)
p_V	vapour pressure (Pa)
Q	ratio of molecular weight of water to that of air (–)
Sh	Sherwood number (–)
t	time (s)
T	temperature (K, °C)
X	moisture content ($kg\,kg^{-1}$)
y	mole-fraction concentration (–)
Y	gas humidity ($kg\,kg^{-1}$)

Greek symbols

β_1, β_2, β_3, β_4	mass-transfer coefficients ($s\,m^{-1}$, $s\,m^{-1}\,kg^{-1}$, $K^{-1}\,s^{-1}$, $kg\,m^{-2}\,s^{-1}$)
ρ	density ($kg\,m^{-3}$)
Φ	characteristic moisture content (–)
Ψ	relative humidity (–)

Subscripts

cr	critical
e	equilibrium
G	dry bulb, bulk gas
ref	reference
S	saturated, above fully wetted surface
wb	wet bulb
W	water
V	vapour

the point (1, 1) at the critical point of transition in drying behaviour and the point (0, 0) at equilibrium.

This representation is attractive because it leads to a simple lumped-parameter expression for the drying rate, namely,

$$N_V = f(\hat{N}_V) = f[\beta_1(p_{VS} - p_{VG})] \quad (3)$$

Here β_1 is the external mass-transfer coefficient ($s\,m^{-1}$), p_{VS} the vapour pressure above a fully wetted surface, and p_{VG} the vapour pressure in the bulk gas.

In particular, the concept of a characteristic drying curve states that the shape of the drying-rate curve for a given material is unique and independent of gas temperature, humidity and velocity. Drying-rate curves for the same material at different operating conditions should be geometrically similar, according to this hypothesis. Eq. (3) has been used extensively as the basis for understanding the behaviour of industrial drying plants owing to its simplicity and the separation of the parameters that influence the drying process: the material itself f, the design of the dryer (β_1), and the process conditions ($p_{VS} - p_{VG}$).

Keey and Suzuki [2] have explored the conditions for which a characteristic curve might apply, using a simplified analysis based on an evaporative front receding through a porous mass. Their analysis shows there is a unique curve when the material is thin and the effective moisture diffusivity is high. Characteristic drying curves might then be expected for small, microporous particles dried individually.

Keey [3] has summarised experimental data for the application of a characteristic drying curve to the drying of loose and particulate materials. The concept was found to work well for modest ranges of air temperature, humidity, and velocity for a number of these materials. Significantly, no characteristic drying curve was observed in the drying of large particles (>20 mm in diameter) [4,5]. With fibrous materials, scatter in drying data may also be attributed to uncertainties in measurement with thin layers of loose stuff [6]. There is, nevertheless, a sufficient body of data to suggest that a characteristic drying curve may be found to describe the drying of discrete particles below 20 mm in diameter over a range of conditions that normally exist within a commercial dryer. The review of Keey [3] includes some agricultural products, and an example of the application of a characteristic drying curve to other agricultural products is given by Laws and Parry [7].

Recently, Fyhr and Kemp [8] compared the characteristic drying curve with a Fickian diffusion model for small particles of softwood, ceramic clay, silica gel and purolit. They concluded that, in most cases, the predictions of the characteristic drying curve were as good as or sometimes even better than those from a diffusion model, lending credibility to the characteristic curve approach.

Some drying kinetics data exist in the literature for milk droplets. In 1976, Keey and Pham [9] analysed the data of Trommelen and Crosby [10] for the drying of 2 μl (about 1.6 mm diameter) milk droplets at air temperatures of 150–155°C, finding that a linear falling-rate curve could be fitted to the drying rates. This analysis, based on data from this one work [10], was used by Keey [3] to support his statement that the linear falling-rate model is applicable to the drying of suspended skim milk concentrate. However, there have been other works on skim milk drying since then that have taken different approaches to modelling the drying kinetics [11–15], and a re-evaluation of the experimental data in these works is necessary.

Ferrari et al. [11] reported the drying kinetics for 10 mm diameter milk droplets immobilised in agar gel at temperatures from 50 to 90°C. The effect of the gel on the drying

kinetics behaviour is not clear, but the data will still be analysed in the next section of this paper. Ferrari et al. used a kinetics model based on Fickian diffusion to fit their measured kinetic data. Straatsma et al. [12,13] also used such a diffusion-based approach to modelling the drying kinetics in their numerical simulations of spray dryer performance.

The drying of skim milk droplets of 3–8 mm in diameter, with initial solids concentrations of 20–40%, air velocities from 0.49 to 0.98 m s^{-1}, air temperatures from 20 to 91°C was studied by Hassan and Mumford [14]. However, in many cases, their data suggest that the droplets were not evaporated to complete dryness, making the subsequent analysis of the measured drying kinetics difficult.

Chen et al. [15] report drying kinetics measurements for 2 mm diameter droplets of skim milk suspended at the end of a fibre at dry-bulb temperatures from 70 to 150°C, wet-bulb temperatures from 7 to 16°C, and air velocities from 1 to 1.3 m s^{-1}. They used a kinetics model based on a receding evaporative plane to fit their data. These data will also be analysed in the following section.

In all these studies, the droplet diameters were around two orders of magnitude larger than those normally seen in spray dryers because of the practical need to perform experiments on droplets giving measurable mass losses. However, based on the assessment of Keey [3] that smaller diameters are likely to improve the applicability of the characteristic drying curve, if the concept applied to these relatively large droplets, then it should apply to the droplets of milk in real spray dryers.

1.1. Analysis of drying kinetics data from previous researchers

The lumped-parameter expression for the drying rate given in Eq. (3) can be rewritten in the following form, for a material with a linear falling-rate curve (relative drying rate f proportional to the free moisture content $(X - X_e)$) and having no constant rate period (so that the drying rate begins to fall immediately from the start of drying):

$$N_V \equiv -\frac{d(X - X_e)}{dt} = (X - X_e)[\beta_2(p_{VS} - p_{VG})] \cong (X - X_e)[\beta_3(T_G - T_{wb})] \quad (4)$$

since the vapour-pressure driving force $(p_{VS} - p_{VG})$ is virtually proportional to the wet-bulb depression $(T_G - T_{wb})$, and the wet-bulb depression can be estimated from the information provided by Chen et al. [15]. Eq. (4) may be integrated between the initial moisture content (X_i) at time $t = 0$ and any moisture content (X) at time t to give

$$\ln\left(\frac{X - X_e}{X_i - X_e}\right) = \beta_3(T_G - T_{wb})t \quad (5)$$

Chen et al. [15] show three drying kinetics curves for skim milk droplets with a solid content of 20 wt.% for dry-bulb temperatures from 70 to 110°C. As shown in Figs. 1–3, these curves can all be fitted (using least-squares) by a value for β_3 of 1.69×10^{-4} K^{-1} s^{-1}. The degree of fit is comparable with that given by the multi-parameter equation, based on a receding evaporative interface, given by Chen et al. Furthermore,

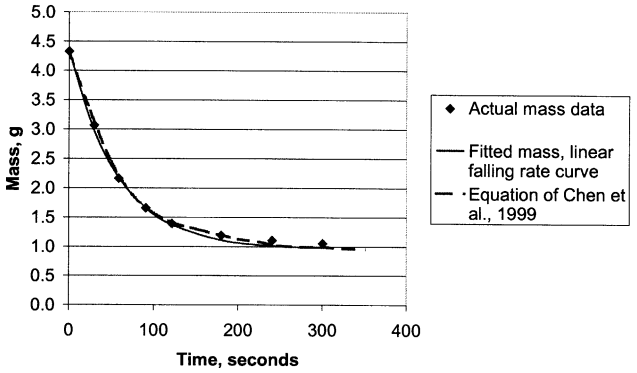

Fig. 1. Comparison of fit given by the linear falling-rate curve with the drying kinetics expression of Chen et al. [15] for a dry-bulb temperature of 110°C, a room temperature of 20°C, a relative humidity at room temperature of 45%, a solids content of 20%, and an air velocity of 1.3 m s^{-1}.

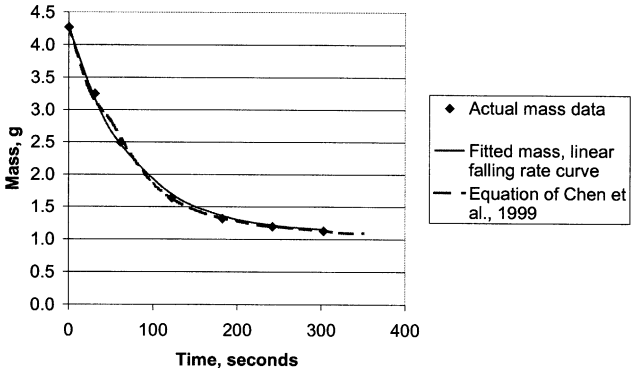

Fig. 2. Comparison of fit given by the linear falling-rate curve with the drying kinetics expression of Chen et al. [15] for a dry-bulb temperature of 90°C, a room temperature of 20°C, a relative humidity at room temperature of 50%, a solids content of 20%, and an air velocity of 1.3 m s^{-1}.

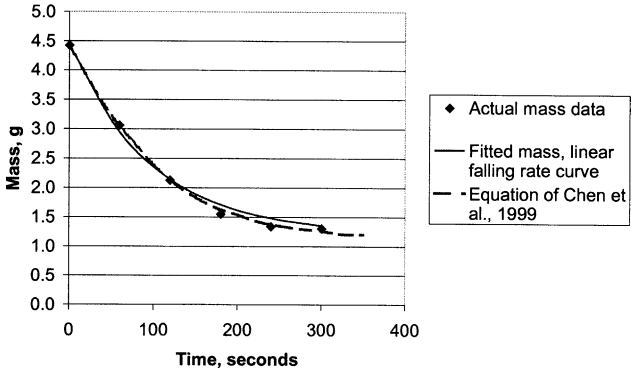

Fig. 3. Comparison of fit given by the linear falling-rate curve with the drying kinetics expression of Chen et al. [15] for a dry-bulb temperature of 70°C, a room temperature of 20°C, a relative humidity at room temperature of 50%, a solids content of 20%, and an air velocity of 1.3 m s^{-1}.

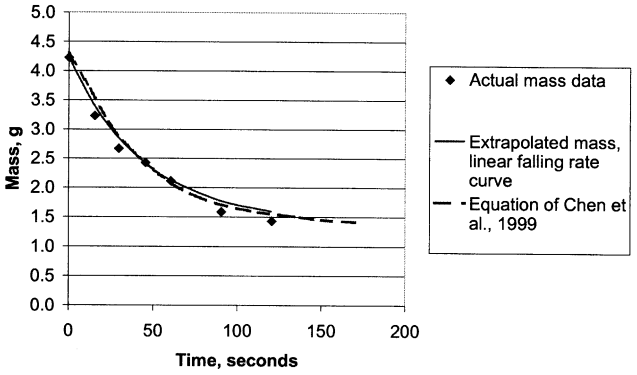

Fig. 4. Comparison of the extrapolated linear falling-rate curve fitted in Figs. 1–3 with the drying kinetics expression of Chen et al. [15] for a dry-bulb temperature of 150°C, a room temperature of 25.5°C, a relative humidity at room temperature of 57%, a solids content of 30%, and an air velocity of $1\,m\,s^{-1}$.

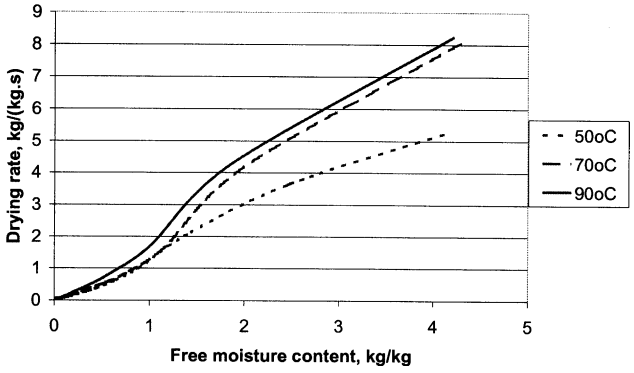

Fig. 5. Drying rate curves extracted from the moisture content against time curves of Ferrari et al. [11] for dry-bulb temperatures from 50 to 90°C.

when this fitted value of β_3 is used to extrapolate the linear falling-rate curve to conditions outside the range (150°C) over which the constant was fitted (70–110°C), the linear falling-rate curve still performs as well as the receding evaporative interface expression, as shown in Fig. 4.

The coefficient (β_3) should be equal to the external heat-transfer coefficient divided by the product of the mass of dry solids per unit surface area, the initial free moisture content (mass of water per unit mass of dry solids) and the latent heat of vaporisation. The latent heat of vaporisation for water is about $2.2 \times 10^6\,J\,kg^{-1}$, the initial free moisture content is $4\,kg\,kg^{-1}$ and the amount of dry milk solids per unit initial volume of droplets is around $250\,kg\,m^{-3}$. Chen et al. [15] state that the particles were approximately 2 mm in diameter, and in view of this approximate figure for the diameter, it is reasonable to fit a heat-transfer coefficient. With these assumptions, the fitted value of the coefficient (β_3) from the data of Chen et al. ($1.69 \times 10^{-4}\,K^{-1}\,s^{-1}$) gives a fitted heat-transfer coefficient of $124\,W\,m^{-2}\,K^{-1}$. This heat-transfer coefficient is reasonable, given the relative velocities between the particle and the air quoted by Chen et al. of $1–1.3\,m\,s^{-1}$, since the Ranz–Marshall equation for these conditions gives heat-transfer coefficients of around $85\,W\,m^{-2}\,K^{-1}$.

Ferrari et al. [11] give no information about the humidity of the air used in their experiments, so it is not possible to estimate the wet-bulb temperatures that they used. Hence their data for moisture contents as a function of time for dry-bulb temperatures between 50 and 90°C have been transformed into drying rate against moisture content curves, as shown in Fig. 5. Although the curves are slightly sigmoidal, the shapes are not highly non-linear, even though the particle diameters used by Ferrari et al. of 10 mm were even larger than those of Chen et al. of 2 mm, and Ferrari et al. used agar gel to immobilise the large drops of liquid milk. Both the experimental data of Ferrari et al. and Chen et al. therefore lend support to the use of a linear falling-rate curve.

2. Theory

The most important outputs from any drying kinetics model are the temperatures and moisture contents of the particles, so the physical approach to implementing the drying model and the particle energy balance will be outlined here.

During drying, the characteristic drying curve means that the mass-transfer rate from particles is reduced below that for unhindered drying if the characteristic moisture content is less than unity, as shown in Eqs. (1) and (2). The approach to estimating the unhindered drying rate is outlined in the next section. For higher characteristic moisture contents, the relative drying rate may be set to unity, while for a moisture content equal to that at equilibrium, the mass-transfer rate is zero since both the free and characteristic moisture contents are also zero.

2.1. Mass-transfer rate for unhindered drying

For mass transfer through the boundary layer above a fixed surface where the solids do not hinder the mass-transfer rate, the integration of Fick's law [16] gives the following equation for the mass-transfer flux:

$$\hat{N}_V = \beta_4 \ln\left(\frac{1 - y_G}{1 - y_S}\right) \tag{6}$$

where y is the mole-fraction concentration and the subscripts S and G refer to the conditions just above the particle surface and in the bulk gas, respectively.

On introducing the particle surface area (A) and the molecular weight of water (M_W), Eq. (6) gives the rate of mass loss from the particle as

$$\frac{dm_W}{dt} = A\beta_4 M_W \ln\left(\frac{1 - y_G}{1 - y_S}\right) \tag{7}$$

Eq. (7) may be rewritten in terms of the particle diameter (d_P), the Sherwood number (Sh), the diffusivity of water vapour through air (D_V) and the vapour density (ρ_V) as

$$\frac{dm_W}{dt} = \pi d_P\, Sh\, D_V \rho_V \ln\left(\frac{1 - y_G}{1 - y_S}\right) \tag{8}$$

This equation can be expressed in terms of gas humidity (mass of water per unit mass of dry gas) as

$$\frac{dm_W}{dt} = \pi d_P Sh D_V \rho_V \ln\left(\frac{Q + Y_S}{Q + Y_G}\right) \quad (9)$$

where Q is the ratio of the molecular weight of water to that of dry air (0.622). The Sherwood number in Eq. (9) and the Nusselt number for heat transfer have both been estimated from the Ranz–Marshall equation [17].

2.2. Particle energy balance

An energy balance for a particle that is drying gives the following equation:

$$m_P C_{PP} \frac{dT_P}{dt} = \pi d_P Nu\, k(T_G - T_P) + H_V \frac{dm_W}{dt} \quad (10)$$

where k is the thermal conductivity of the gas and H_V the latent heat of vaporisation for water.

2.3. Equilibrium moisture content

For predicting the equilibrium moisture content of skim milk powder, Stafford [18] identified parameters in an equation of the form:

$$X_e(T, \Psi) = X_e(T_{ref}, \Psi) \exp[-B(T - T_{ref})] \quad (11)$$

where Ψ is the relative humidity. For the term $X_e(T, \Psi)$, which represents the behaviour at a reference temperature (T_{ref}), the following equation, proposed by Halsey [19], was used:

$$X_e(T_{ref}, \Psi) = K_1(\ln \Psi)^{K_2} \quad (12)$$

Here, K_1 and K_2 are the constants at a particular temperature. Stafford [18] reviewed equilibrium moisture content data for skim milk powder at 14, 34 and 45°C. At a temperature of 34°C, two data sets were found, and these agreed well over a relative humidity range from 0 to 80%. In this work, since the particle temperatures are usually above 50°C, values of the constants obtained by Pixton [20] at 45°C (the highest temperature, used here as the reference temperature, T_{ref}) have been used ($K_1 = 0.047$ and $K_2 = -0.787$).

In Eq. (11), Stafford [18] proposed that the parameter B should be proportional to the relative humidity, varying from 0.012 to 0.0215 as the relative humidity increases from 0.1 to 0.5. The basis of this proportionality was not clear, and the treatment of conditions outside this range of relative humidities was also not specified.

3. Discussion

This theory has been assessed for a particle with an initial diameter, velocity, temperature and moisture content of 80 μm, 0 m s^{-1}, 293 K and 1 kg kg^{-1}, respectively. The particle size of 80 μm is representative of particle sizes seen in spray dryers [21]. The gas conditions included dry and wet-bulb temperatures of 353 and 305 K, respectively, and a velocity of 10 m s^{-1}. The coefficient (β_3) in Eq. (5) was estimated to be 0.084 K^{-1} s^{-1} for this situation, from the external heat-transfer coefficient divided by the product of the mass of dry solids per unit surface area, the initial free moisture content and the latent heat of vaporisation. From the Ranz–Marshall equation, the heat-transfer coefficient was estimated as 1340 W m^{-2} K^{-1}, and an 80 μm diameter particle has a surface area of 75,000 m^2 m^{-3}. Then, from the coefficient β_3, the wet-bulb depression of 50 K and the initial moisture content of 1 kg kg^{-1}, the drying behaviour has been calculated and is shown in Fig. 6. A significant feature is that the drying of this 80 μm particle is virtually complete within 1 s, which is short compared with typical residence times inside spray dryers (from 20 to 80 s [21]).

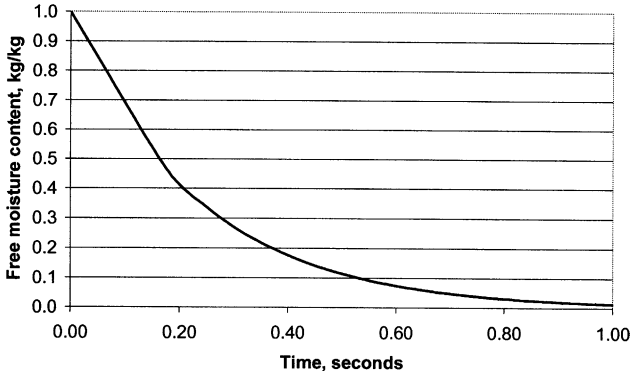

Fig. 6. Calculated free moisture content (actual moisture content − equilibrium moisture content) as a function of time for a particle with an initial diameter, velocity, temperature and moisture content of 80 μm, 0 m s^{-1}, 293 K and 1 kg kg^{-1}, respectively, in air with dry- and wet-bulb temperatures of 353 and 305 K, respectively, and an air velocity of 10 m s^{-1}.

The use of a characteristic drying curve (which involves only the average moisture content) has some disadvantages, since strictly speaking, the moisture content at the surface of the powder governs the fouling of spray dryer walls. However, the calculation of local moisture contents within particles is currently impractical with CFD calculations of transient, three-dimensional flow patterns in spray dryers. Such flow patterns have been shown to be key features of the performance of these dryers [22]. In addition, the short drying times shown here for particles of the size typically encountered in spray dryers, compared with the residence times of particles, mean that the particles are essentially in equilibrium with the gas, so for the purposes of estimating wall deposition, the moisture gradients are likely to be small.

4. Conclusions

A linear falling-rate curve is an acceptable approximation for the hindered drying of milk powder, as shown by a review

of previous literature where particle diameters have been greater than 2 mm. For the diameters of milk particles in spray dryers, the drying times are predicted using a linear falling-rate curve to be of the order of 1 s, compared with residence times of 20–80 s in full-scale equipment. Such a model is in a form which can be, and indeed has been, used in a CFD model to predict particle behaviour in milk spray dryers.

Acknowledgements

The support of the Dairy Research and Development Corporation for this work is gratefully acknowledged.

References

[1] R.E. Bahu, in: A.S. Mujumdar, I. Filkova (Eds.), Spray drying — maturity or opportunities? Drying'92, Elsevier, Amsterdam, 1992, pp. 74–91.
[2] R.B. Keey, M. Suzuki, On the characteristic drying curve, Int. J. Heat Mass Tran. 17 (1974) 1455–1464.
[3] R.B. Keey, Drying of Loose and Particulate Materials, Hemisphere, New York, 1992.
[4] M. Haertling, E.U. Schlünder, Prediction of drying rates, J. Separ. Proc. Technol. 1 (1980) 47–50.
[5] W. Schicketanz, Vergleich des trocknungsverhaltens von schüttungen kapillärporöser materialen (Comparison of the drying process of beds of capillary-porous materials), Chem. Ing. Tech. 43 (1980) 245–251.
[6] R.B. Keey, Y. Wu, An analysis of the suction-drum drying of wool, in: Proceedings of the Fourth Australasian Conference on Heat Mass Transfer, Christchurch, New Zealand, 1989, pp. 217–225.
[7] N. Laws, J.L. Parry, Mathematical modelling of heat and mass transfer in agricultural grain drying, Proc. R. Soc. London A 385 (1983) 169–187.
[8] C. Fyhr, I.C. Kemp, Comparison of different drying kinetics models for single particles, Dry. Technol. — Int. J. 16 (7) (1998) 1339–1369.
[9] R.B. Keey, Q.T. Pham, Behaviour of spray dryers with nozzle atomizers, Chem. Engr. 311 (1976) 516–521.
[10] A.W. Trommelen, E.J. Crosby, Evaporation and drying of drops in superheated vapour, Am. Inst. Chem. Engrs. J. 16 (5) (1970) 857–866.
[11] G. Ferrari, G. Meerdink, P. Walstra, Drying kinetics for a single droplet of skim milk, J. Food Eng. 10 (1989) 213–222.
[12] J. Straatsma, G. Van Houwelingen, A.E. Steenbergen, P. De Jong, Spray drying of food products: 1. Simulation model, J. Food Eng. 42 (2) (1999) 67–72.
[13] J. Straatsma, G. Van Houwelingen, A.E. Steenbergen, P. De Jong, Spray drying of food products: 2. Prediction of insolubility index, J. Food Eng. 42 (2) (1999) 73–77.
[14] H.M. Hassan, C.J. Mumford, Mechanisms of drying of skin-forming materials. III. Droplets of natural products, Dry. Technol. — Int. J. 11 (7) (1993) 1765–1782.
[15] X.D. Chen, M. Farid, D. Reid, A. Fletcher, D. Pearce, N.X. Chen, A new model for the drying of milk droplets for fast computation purposes, in: Proceedings of the Chemeca'99, Newcastle, Australia, 1999, pp. 825–830.
[16] R.E. Treybal, Mass-Transfer Operations, McGraw-Hill, New York, 1980, pp. 47–48.
[17] W.E. Ranz, W.R. Marshall, Evaporation from drops, Chem. Eng. Progr. 48 (3) (1952) 141–146, 173–180.
[18] R.A. Stafford, A temperature dependent equilibrium moisture content expression, Milk Sci. Int. 48 (7) (1993) 371–373.
[19] G. Halsey, Sorption equilibria, J. Chem. Phys. 16 (1948) 931–933.
[20] S.W. Pixton, The importance of moisture and equilibrium relative humidity in stored products, Trop. Stored Prod. Inf. 43 (1982) 16–29.
[21] K. Masters, Spray Drying Handbook, Halstead Press, New York, 1992.
[22] D.B. Southwell, T.A.G. Langrish, Observations of flow patterns in a spray dryer, Dry. Technol. — Int. J. 18 (3) (2000) 661–685.